Quantitative analysis of surface coseismic faulting and postseismic creep accompanying the 2003, M_w = 6.5, Chengkung earthquake in eastern Taiwan

Jian-Cheng Lee,[1] Hao-Tsu Chu,[2] Jacques Angelier,[3] Jyr-Ching Hu,[4] Horng-Yue Chen,[1] and Shui-Beih Yu[1]

[1] On the basis of field observations and geodetic measurements we analyzed coseismic and postseismic deformation of the 2003, M_w = 6.5, Chengkung earthquake across the rupture trace of the Chihshang fault, which lies along the suture zone between the Philippine Sea plate and the Eurasian plate in eastern Taiwan. At three of our investigation sites along the Chihshang fault the earthquake deformation was exhibited by fresh fractures within the 150- to 200-m-wide surface fault zone, reactivating preexisting fractures in most cases. In addition to daily recorded creep meter data, geodetic measurements, including leveling, distance-and-angle electronic distance meters, and GPS measurements, were carried out during surveys 20–25 days before, 20–25 days after, and 120–125 days after the earthquake. The near–fault surface deformation is mainly characterized by anticlinal folding in the hanging wall and minor gentle synclinal folding in the footwall. The geodetic data show that within our 150- to 250-m-wide networks the coseismic deformation of the main shock produced only about 1–2 cm of horizontal shortening and vertical offset across the fault zone. A larger additional displacement of about 7–9 cm for both the horizontal shortening and the vertical offset occurred as postseismic creep during the 120–125 days following the main shock. We interpret the predominant folding and the rather large postseismic creep as a result of strong velocity strengthening along the fault plane near the surface, which caused locking or coupling effect during the coseismic rupturing. The depth of locked segment, along which the coseismic and postseismic slip decreased dramatically upward, is estimated to be 25–100 m, depending on the site. We interpreted the velocity strengthening and coupling effect at the shallow level as viscoelastic behavior of unconsolidated deposits in the footwall and mélange mudstone in the hanging wall. By incorporating far-fault continuous GPS data, it was found that minor but significant deformation occurred outside of the surface ruptures zone of the Chihshang fault. In addition, a possible back thrust or back fold might have occurred in the hanging wall. We note that the Chengkung earthquake occurred during the dry season. This is consistent with the fact that the mechanical coupling of the fault at shallow depth is higher during drier periods, inferred from the previous seasonal creep data. At outcrop scale, regarding damage of construction such as a concrete retaining wall, most of the coseismic and postseismic horizontal shortening was essentially absorbed by multiple distributed brittle ruptures, which deserves attention in terms of earthquake hazard mitigation.

[1]Institute of Earth Sciences, Academia Sinica, Taipei, Taiwan.
[2]Central Geological Survey, Taipei, Taiwan.
[3]Géosciences Azur, Observatoire Océanologique de Villefranche, Villefranche-sur-Mer, France.
[4]Department of Geosciences, National Taiwan University, Taipei, Taiwan.

1. Introduction

[2] The Chengkung earthquake of magnitude M_w = 6.5 occurred in eastern Taiwan on 10 December 2003, resulting from rupture of the Chihshang fault (Figure 1). The focus of the earthquake was at a depth of about 20 km, with the epicenter near the coastal town of Chengkung, about 16 km east of the surface trace of the Chihshang fault. The damage caused by the Chengkung event was moderate, albeit not
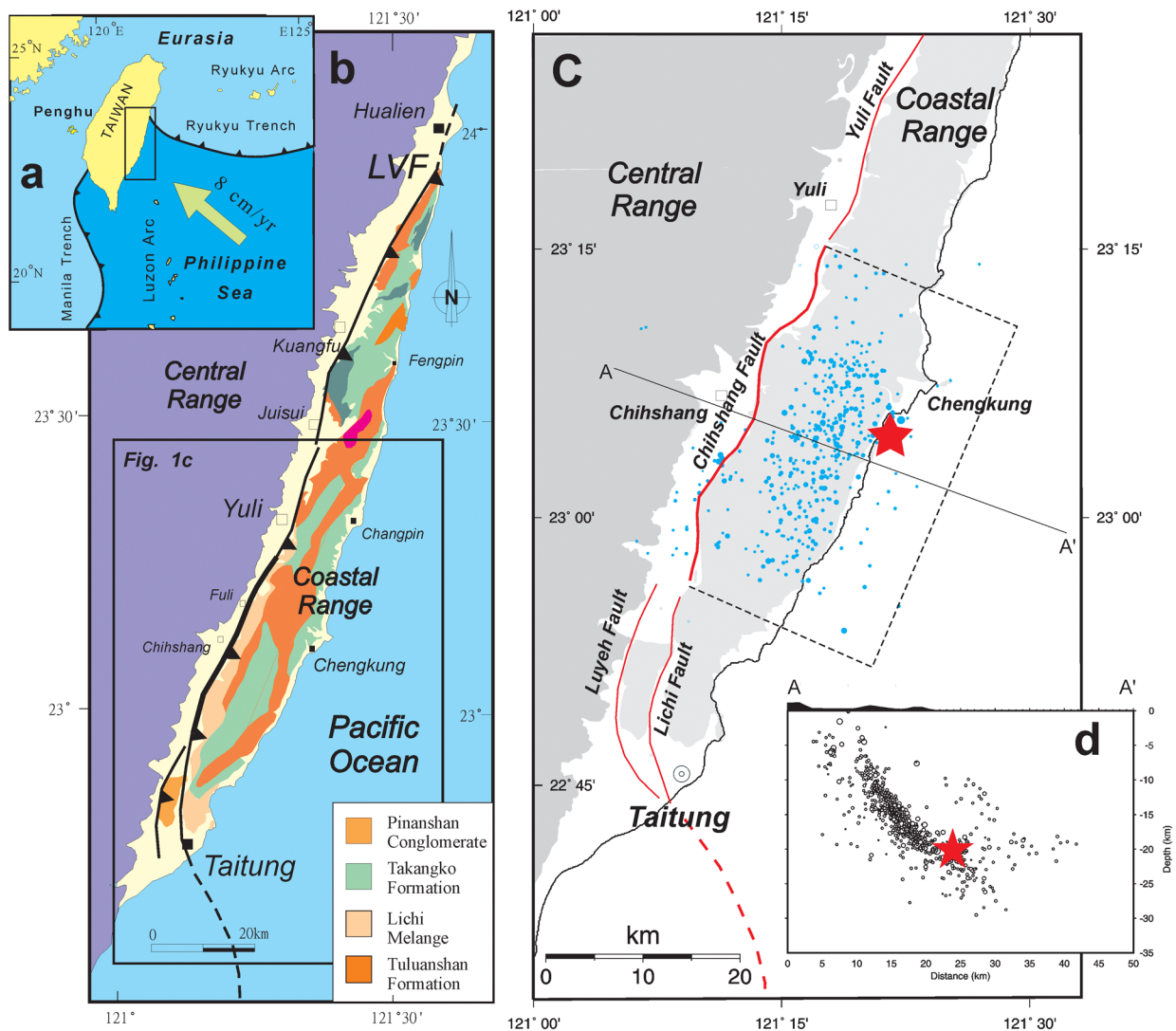
Figure 1. (a) Plate-tectonic setting of Taiwan. (b) General geology of the Coastal Range. The Coastal Range is thrust onto the Longitudinal Valley and the Central Range along the active Longitudinal Valley fault (LVF) (heavy line with triangles pointing in dip direction). (c) Seismicity map of main shock (star) and aftershocks (dots) of the 2003 M_w 6.5 Chengkung earthquake. (d) Cross section of the distribution of the 2003 earthquake sequence.

severe, including large numbers of fissures in man-made structures and a few landslides not only near the epicenter but also along the surface trace of the Chihshang fault. Numerous aftershocks occurred during several weeks following the main shock. This earthquake sequence, including the main shock and most of the aftershocks, was distributed mainly along the NNE striking and east dipping Chihshang fault (Figure 1), forming a patch approximately 35 km long (along strike) and 20 km wide (in the downdip direction) [Ching et al., 2004].

[3] The Chihshang fault and its northern neighbor, the Yuli fault (Figure 1), previously ruptured during an earthquake sequence in 1951, with tens of centimeters of vertical offset along the Chihshang fault and 1–1.5 m of vertical and horizontal offsets along the Yuli fault [Bonilla, 1975; Yü et al., 1997; Chung et al., 2002]. These two faults, especially the Chihshang fault subsequently underwent continuous surface creep, which caused cracks in con-

structions, such as retaining walls and concrete water channels, during the last 20 years [Barrier and Chu, 1984; Lee, 1994; Angelier et al., 1997]. Creep along the Chihshang fault is similar to that on the creeping segment of the San Andreas Fault north of Parkfield. During the past two decades, different monitoring efforts have been undertaken across the Chihshang fault at different spatial and temporal scales. These include GPS (both campaign and continuous modes) [Yu et al., 1997; Yu and Kuo, 2001], trilateration networks [Yu and Liu, 1989; Lee et al., 2003b], leveling [Yu and Liu, 1989; Lee et al., 2003b], measurements of offset of fractures on surface construction [Angelier et al., 1997, 2000], and creep meter surveys [Lee et al., 2001, 2003a]. Previous measurements indicated a rapid creeping rate of about 2–3 cm/yr. The Chihshang fault is probably one of the most rapidly creeping thrust faults known to exist. Furthermore, the variety of instrumentation across the Chihshang fault provides an opportu-
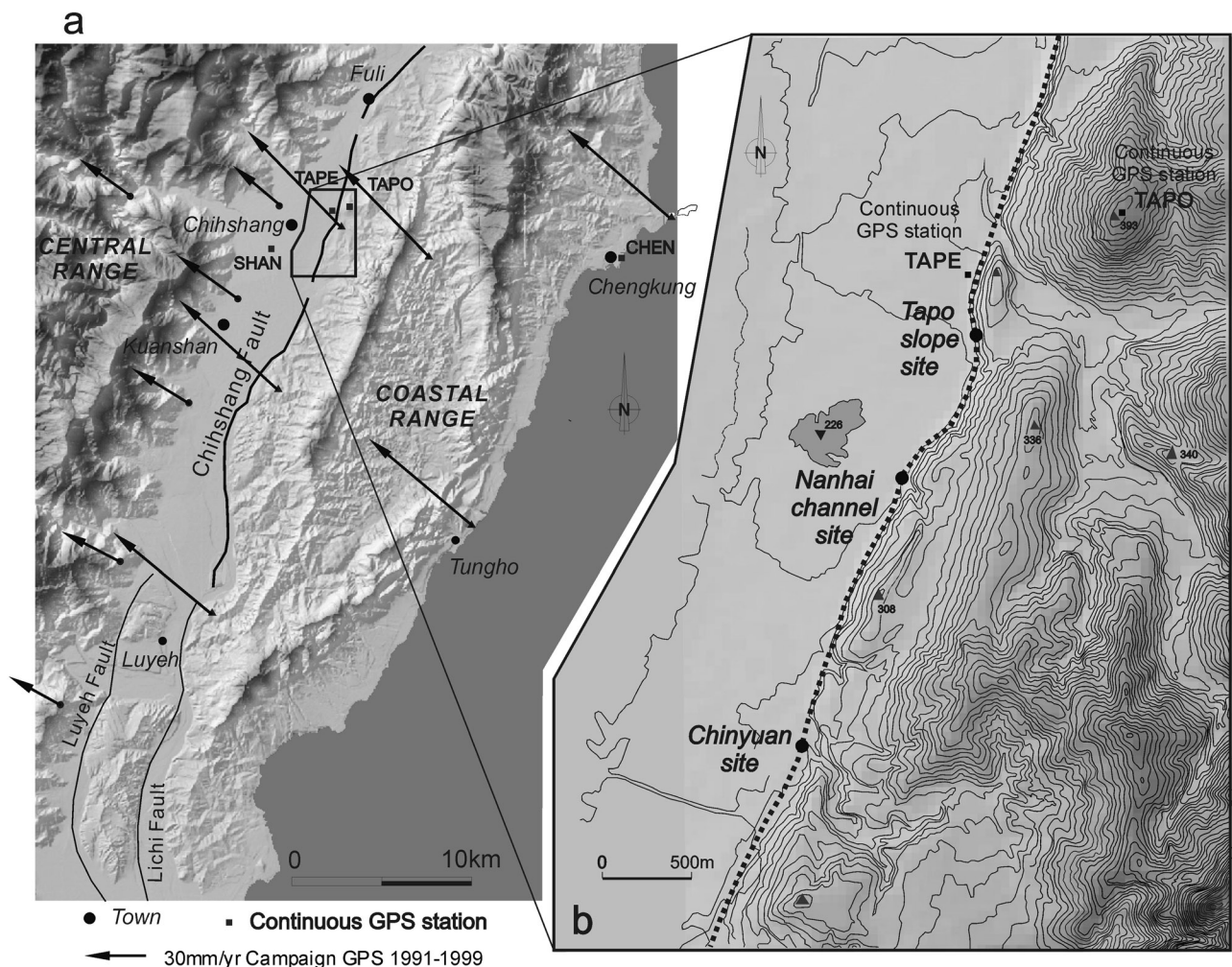
Figure 2. General morphologic features of the active Chihshang fault and location of geodetic networks. (a) Shaded relief (light from northwest) from 40-m digital elevation model and campaign GPS displacements during 1991–1999 (after *Yu et al.* [1997] and *Yu and Kuo* [2001]). The GPS vectors are with respect to a continuous GPS station at Penghu Islands in Taiwan Strait (location see Figure 1a). Three nearby GPS continuous stations, SHAN, TAPE, and TAPO, are also shown. (b) Site map with topographic contours showing the scarps of the Chihshang fault. The three black dots indicate sites of the geodetic network.

nity for comprehensive quantitative analysis of the surface deformation, both interseismic and coseismic.

[4] In this paper, we seek to quantify surface deformation associated with the 2003 earthquake along the Chihshang fault. We focus on three sites near the town of Chihshang, where dense geodetic networks have been set up, and systematic observations and measurements on rupture traces have been carried out during the past few years. At each site, we show the results of the measurements of earthquake-related displacement. We describe quantitatively the surface deformation patterns and discuss probable kinematics of faulting at surface level. We find that most of the displacement occurs by postseismic creep and only a small portion is due to coseismic rupture. The reasons behind the occurrence of little coseismic slip compared with more significant postseismic creep are discussed with regard to their geological implications, especially strong velocity strengthening of fault and viscoelastic effect due to uncon-

solidated deposits at shallow level. We also define how the variation in deformation from site to site can be interpreted in terms of local geological site effects.

2. Seismotectonic Framework

[5] The Chihshang fault forms the central part of the southern segments of the Longitudinal Valley fault (LVF), a suture between the Philippine Sea plate and Eurasian plate in eastern Taiwan (Figure 1). The suture formed as the Luzon arc of the Philippine Sea plate (i.e., the Coastal Range) collided with the Eurasian continental margin, starting about 5 Myr ago [*Ho*, 1986; *Teng*, 1990] and is still active presently [*Tsai*, 1986; *Suppe*, 1984; *Yu et al.*, 1997]. GPS measurements across the plate suture during 1991–1999 (Figure 2) indicate that surface deformation occurs along the LVF at a horizontal shortening rate of about 3 cm/yr [*Yu and Kuo*, 2001], compared to 8 cm/yr

across the whole mountain belt [*Yu et al.*, 1997]. In the southern part of the Longitudinal Valley, the rate of convergence as defined by geodesy is mirrored by high microseismic activity along the Chihshang fault, as revealed by the Central Weather Bureau (CWB) seismic network operating in the Taiwan area since 1990 [*Chen and Rau*, 2002]. In summary, most of the shortening that occurs across the plate suture in the southern Longitudinal Valley and Coastal Range is mainly concentrated across a single fault, the Chihshang fault [*Lee and Angelier*, 1993; *Angelier et al.*, 1997; *Lee et al.*, 2003a].

[6] The Chihshang fault is marked by topographic scarps along the base of the rugged Coastal Range, where rocks of the Luzon arc are exposed (Figure 2). The Lichi Mélange (clay matrix with a variety of exotic blocks) of the Coastal Range is thrust over Holocene alluvial deposits across the Chihshang fault in the Longitudinal Valley. An exposure of the Chihshang fault is preserved along a riverbank south of the town of Fuli [*Angelier et al.*, 2000]. Fault scarps several meters in height deform fluvial terrace deposits in a number of locations along the range front of the Coastal Range. The most visible surface features that record recent slip on the Chihshang fault are abundant fractures in man-made structures. In particular, thrust-type fractures with progressive displacement in concrete retaining walls reveal the movements of tectonic origin and allow surface fault deformation to be measured. Previous studies have described these surface features in detail [e.g., *Barrier and Chu*, 1984; *Chu et al.*, 1994; *Lee*, 1994; *Angelier et al.*, 1997, 2000], and also documented recent and rapid creep of surface fractures of the Chihshang fault during the last 20 years. Although soil creep down the scarp of the fault cannot be totally excluded, fractures caused by lateral spreading of gravitational instability generally can be easily identified because of their extensional characteristics [*Angelier et al.*, 2000]. In addition, comparison of measurements from different sites to sites on flat alluvial deposits [*Angelier et al.*, 2000; *Lee et al.*, 2003a] indicate that gravitational effects and surface soil downslope creep were very limited at selected measurement sites.

3. Field Investigation and Quantitative Analyses

[7] Since 1990, we have carried out an increasing variety of measurements for quantifying surface deformation at several selected sites in the Chihshang area (Figure 2), where the motion of the Chihshang fault was clearly detectable. For example, networks of nails hammered in concrete walls across fractures were measured to define movement across these features since 1992 [*Lee*, 1994; *Angelier et al.*, 1997, 2000]. We also deployed several small geodetic networks (about 150–250 m wide and long) across surface rupture zone of the fault at three sites: Tapo slope, Nanhai channel, and Chinyuan (Figure 2b). Leveling, GPS, and trilateration angle-and-distance measurements using electronic distance meters (EDM) were carried out on these networks once or twice per year since 1998 [*Lee et al.*, 2003b]. Furthermore, in 1998, we installed rod-type creep meters straddling the surface traces of the Chihshang fault to monitor the surface fault motion in a near-continuous manner [*Lee et al.*, 2003a].

[8] After the 10 December 2003 Chengkung earthquake, we performed repeated measurements at those sites that had already been analyzed before this earthquake. Leveling, GPS, and trilateration network EDM measurements were deployed twice following the main shock: first in late December 2003 to early January 2004 and second in mid-April 2004. In order to reconstruct the deformation resulting from the Chengkung earthquake, the geodetic data collected were compared to those available in mid-November 2003, less than 1 month before the Chengkung earthquake. We thus obtained good temporal resolution for determining the surface deformation associated with the 2003 Chengkung earthquake. The data show that a significant amount of slip occurred during a period of at least 4 months following the main shock, which is an indication of significant postseismic slip. Without repeated surveys, this slip would have probably been attributed to purely coseismic rupturing.

[9] For leveling measurements, we used a Zeiss DiNi 11T leveling instrument with a pair of invar rods. Our measurements used first-order (class I) standards according to the U.S. National Geodetic Survey [*Schomaker and Berry*, 1981]. Standard errors in the double-run leveling are expected to be less than 1.0 mm $\times$ $s^{1/2}$, where s is the survey distance in km (in this study, typically 10–50 m). For the trilateration angle-and-distance measurements, a Trimble 5600 GDM (Geodimeter) total station was used. The standard deviation is about 1.0 mm for distance and 1.0 s for angle at a distance of 100 m. Trimble GPS instruments were used in the GPS campaign measurements with an observed time of 6–8 hours for each station. We used as a base station a continuous GPS station located nearby in the town of Chihshang (SHAN in Figure 2a) for calibration and to calculate the relative displacements for each measured benchmark. The horizontal standard deviation of the GPS displacement was estimated to be about 1 cm for our campaign measurements. The vertical standard deviation of GPS displacements is about 3–4 times that of the horizontal ones. For the creep meter measurements, the technical precision of our self-developed rod-type creep meters for measuring distance changes is about 0.1 mm after thermal calibration [*Lee et al.*, 2001, 2003a].

4. Tapo Slope Site

4.1. Observations Prior to the Chengkung Earthquake and Installation of Geodetic Network

[10] The Tapo slope site is located mainly along a road climbing up the slope along the edge of the frontal hills of the Coastal Range (Figures 2 and 3). The surface trace of the Chihshang fault is approximately at the foot of the slope. Slip along the fault had broken a retaining wall at the side and had caused two thrust-type fractures. These fractures crept about 2.5–2.7 cm/yr during 1986–1994 [*Angelier et al.*, 1997]. However, a more resistant concrete wall had been built in 1994 to replace the old wall. The new wall apparently has prevented surface breakage at the Tapo slope along the creeping Chihshang fault, until the Chengkung earthquake in late 2003.

[11] In 1998, we set up a simple geodetic network across the Tapo slope, with five benchmarks. In 2001, we added seven benchmarks to complete the network, which com-
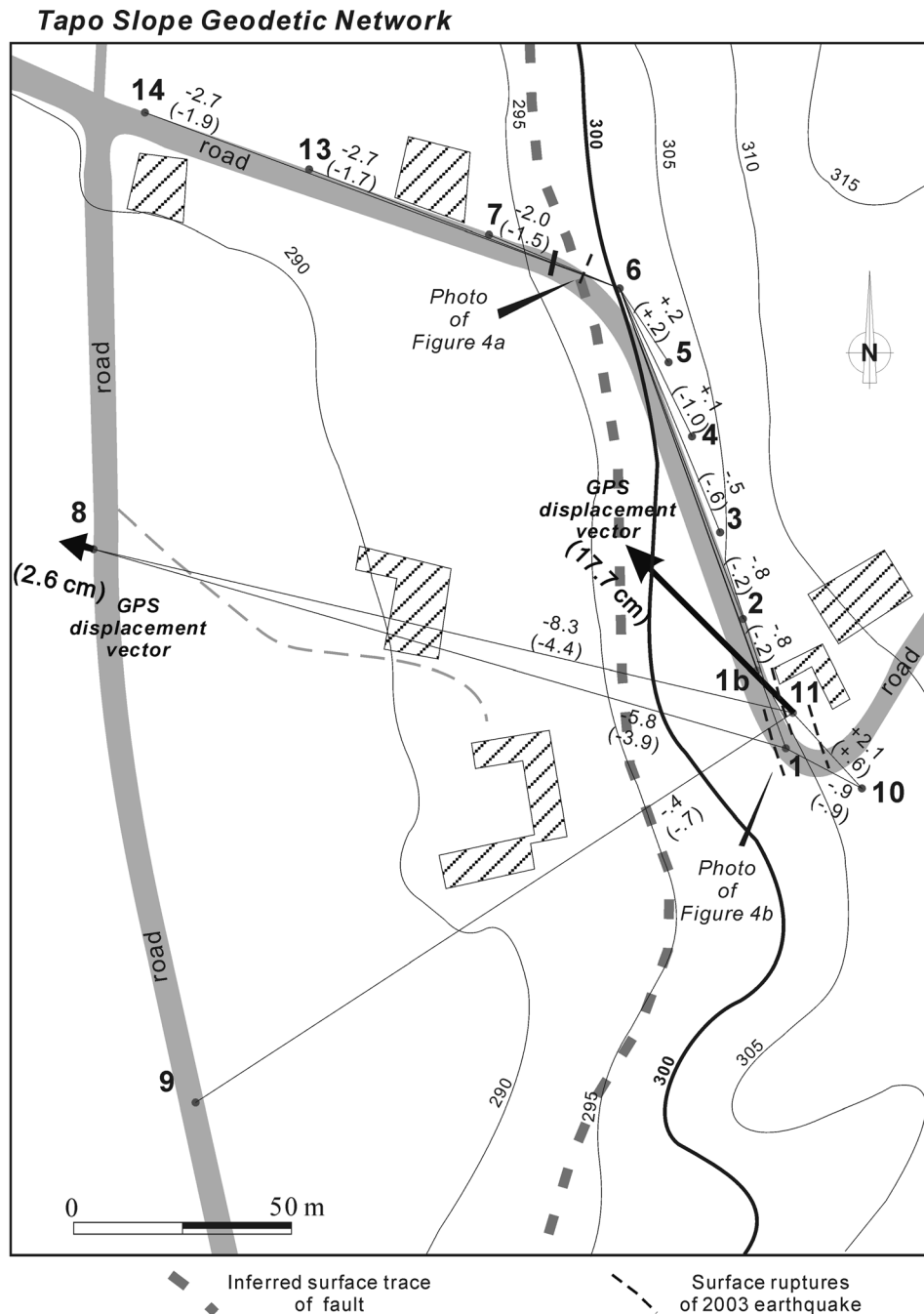
Figure 3. Geodetic network at the Tapo slope site. The contours show the 15- to 20-m-high scarp of the Chihshang fault. The values between the baselines represent the change of distance in millimeters between the benchmarks (numbered in bold) during the first period of the measurements and those through two periods (values in parentheses); positive value equals elongation, and negative value indicates shortening. The GPS displacement vectors represent movement of benchmarks with respect to the continuous GPS station SHAN in the footwall. Polygons with diagonal pattern are buildings.

prised 12 benchmarks distributed across the 20-m-high scarp that extended from the footwall to the hanging wall over a distance of 180 m (Figure 3). Leveling and distance-angle EDM measurements were completed once or twice a year at the site since 1998. GPS measurements for two benchmarks (points 8 and 11) were also carried out during each survey. The previous results of geodetic measurements from 1998 to 2003 implies a continuous reverse fault–type

creep at a horizontal shortening rate of 2.0 cm/yr and a vertical uplifting rate of 1.8 cm/yr without causing significant surface breaks [Lee et al., 2003b].

4.2. Deformation of the Chengkung Earthquake

[12] While investigating the surface effects of the 2003 Chengkung earthquake 3 weeks after the main shock, we observed fresh ground ruptures at the site of Tapo slope.

a *Compression fractures due to 2003 earthquake at the Tapo slope site*

b *Transtension fractures due to 2003 earthquake at the Tapo slope site*

Figure 4. Photographs of the surface ruptures of concrete pavement along the roadside caused by the 2003 Chengkung earthquake at the Tapo slope site. (a) Pop-up-type or reverse fault–type fractures that indicate compression or shortening. (b) Open en échelon fissures (indicated by arrows) that show transtension from near the top of the geomorphic scarp.

Table 1. Results of Near-Fault Vertical and Horizontal Displacements due to the 2003 Chengkung Earthquake Obtained From Geodetic Measurements at the Three Networks Across the Chihshang Fault Zone[a]

	Tapo Slope (Points 8–1b)		Nanhai Channel (Points Z–I)		Chinyuan (Points I–A)	
	V, cm	H, cm	V, cm	H, cm	V, cm	H, cm
First period[b]	6.5	8.3	6.4	5.7	3.5	3.0
Second period[c]	4.2	4.4	4.6	5.0	3.0	4.3
Total	10.7	12.7	11.0	107	6.5	7.0

[a]Maximum displacements (V is the maximum vertical offset, and H is the maximum horizontal displacement) across the fault zone are indicated. Vertical displacements are obtained from leveling measurements. Horizontal values are derived from distance measurements and GPS measurements.
[b]First period is from 15 November 2003 to 31 December 2003 for the vertical displacements and from 18 November 2003 to 5 January 2004 for the horizontal displacements.
[c]Second period is from 31 December 2003 to 9 April 2004 for the vertical displacements and from 6 January 2004 to 12 April 2004 for the horizontal displacements.

The most visible ruptures, with offsets of a few centimeters, affected the concrete pavement on the roadside at the base of the newly built wall (Figure 4a), which is near the foot of the slope and the surface trace line of the Chihshang fault. Furthermore, transtensional en échelon vertical cracks developed in the asphalt road near the top of the slope (Figure 4b). These cracks probably resulted from oblique extension at the periphery of the near-top flexure [*Philip et al.*, 1992] because of surface deformation of the earthquake.

[13] To facilitate discussion of the progressive deformation related to the 2003 earthquake, we describe the results of our measurements in two periods, in the order they were surveyed. Our first surveys after the 10 December earthquake were conducted 20–26 days after the main shock (on 30 and 31 December 2003 for leveling and 5 and 6 January 2004 for EDM and GPS measurements). The second surveys were conducted 120–125 days after the earthquake (on 9–12 April 2004 for leveling and 12–14 April 2004 for EDM and GPS measurements). The results of these two postearthquake surveys were compared with preearthquake surveys carried out in mid-November (on 11–14 November 2003 for leveling and 16 and 17 November 2003 for EDM and GPS measurements).

[14] Not surprisingly, the earliest measurements following the earthquake revealed significant amounts of slip, both vertical and horizontal, across the Chihshang fault zone at the Tapo slope site. By taking the westernmost benchmark point 8 on the footwall as the fixed reference point (Figure 3), we obtained a maximum horizontal displacement of 8.3 cm and a maximum vertical displacement of 6.5 cm near the top of the scarp (Table 1) for the first period of the measurements. The second measurements of geodetic network indicate significant amounts of postseismic slip: 4.4 cm and 4.2 cm for maximal horizontal and vertical displacements, respectively. The maximum total displacements for two periods across the fault zone were 12.7 cm and 10.7 cm, for the horizontal shortening and the vertical offset, respectively.
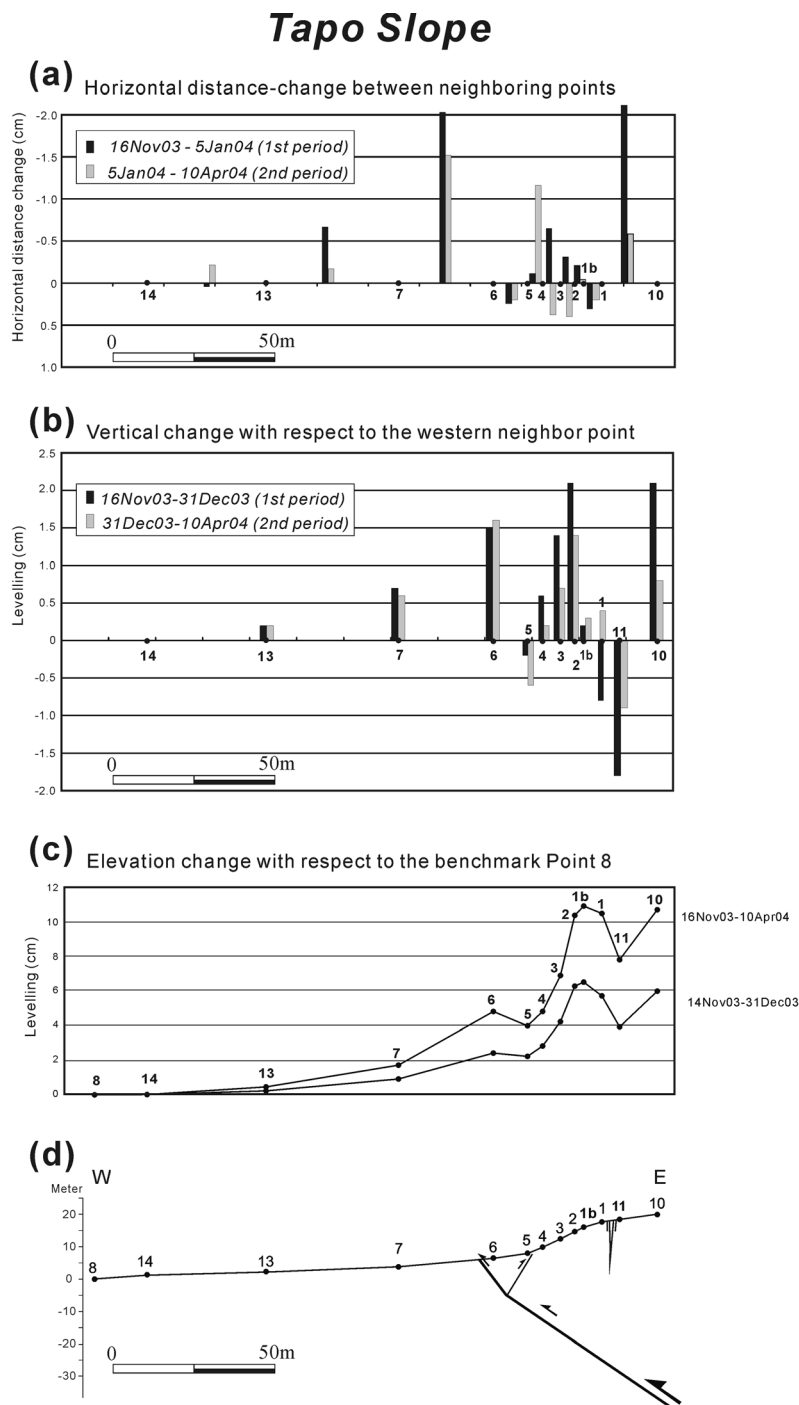
[15] The measurements also reveal the following characteristics. With respect to the westernmost benchmark point 8 on the footwall, the measured displacements for each benchmark increased gradually and rapidly across the fault zone (Figures 3 and 5). The amount of vertical movement was similar to the horizontal movement. There was significant postseismic slip during at least the first 4 months after the 10 December 2003 earthquake.

Differences in deformation between the first (3 November to 3 December) and second (4 January to 4 April) periods at Tapo slope (compare black and grey bars in Figure 5) were (1) subsidence of point 1 was observed relative to the neighboring points only during the first period, (2) larger horizontal shortening was observed between points 5 and 4 during the second period, and (3) extension occurred instead of shortening from point 4 to 1b for the second period.

[16] Combining the results from field observations and geodetic measurements, we conclude that anticlinal fold in the hanging wall is the predominant deformation structure across the Chihshang fault. As a result, we infer that the near-surface fault plane was partially locked or coupled during the 2003 Chengkung earthquake. This explains why deformation (for both the horizontal and the vertical components) increases continuously toward the hanging wall, except for point 5, which records back folding (Figure 5). The trend of elevation changes (Figure 5c) is qualitatively in agreement with an elastic dislocation model of a half-space [e.g., *Savage*, 1983], with a strongly coupled shallow segment. The tip of the main fault would be near the point 6 benchmark. According to previous study of the elastic model in the thrust fault, the depth of the coupled (or locked) segment, on which the fault slip decreased significantly upward, approximately corresponds to the vertical projection from the highest point of elevation change on surface [e.g., *Thatcher and Rundle*, 1979; *Savage*, 1983; *Cattin and Avouac*, 2000]. In the case of Tapo slope, the elevation changes across the fault zone increased dramatically from the fault surface tip to the benchmark 1b. On the basis of a simple vertical projection from benchmark 1b, we estimated the depth of the coupled segment at Tapo slope to be about 20–30 m below the surface (Figure 5). Thus the deformation above the depth of coupled segment was mainly accommodated by tilting or folding, mostly on the hanging wall, instead of rigid block faulting. The near-surface folding during the 2003 event not only produced subtle fold structures in man-made retaining walls, but also brittle ruptures, mostly near the tip of the fault, especially near the junction of two different civil structures, where resistance was less. Detailed kinematic analyses regarding the fault structures and the slip distribution on the fault are beyond the scope of this paper and will be presented elsewhere.

[17] Concrete retaining walls respond to vertical uplift and horizontal shortening in different ways. Most of the

Tapo Slope

(a) Horizontal distance-change between neighboring points

(b) Vertical change with respect to the western neighbor point

(c) Elevation change with respect to the benchmark Point 8

(d)

Figure 5. Results of distance-angle and leveling measurements across the surface fault zone of the Chihshang fault and geological interpretation at Tapo slope site. Position of each benchmark is projected to a cross section perpendicular to the fault strike. (a) Horizontal distance change between neighboring points. Horizontal distance change is a measure between two neighboring points. (b) Vertical change between benchmarks. Vertical change for a benchmark is represented by the relative vertical change with respect to its neighboring point on the western side. (c) Elevation changes or vertical movements of benchmarks with respect to the westernmost point 8. (d) Cross section showing surface ruptures, geometry of the fault, and slip model at the surface level.

horizontal shortening was concentrated and absorbed by brittle ruptures (i.e., between points 6 and 7, and between points 1 and 10, Figure 5a). Vertical uplift was accommodated mostly by folding. In addition to the principal fault, a

back fold and perhaps a back thrust occurred near point 5, especially those from the second period (Figure 5b). We interpret the back fold to be related to an increase of the dip angle of the main fault, which may steepen above 5–8 m in

Figure 6. Results of horizontal distance changes and GPS horizontal displacements that occurred during the 2003 Chengkung earthquake at the Nanhai channel site. The contour lines show that the site is located across the scarp of the Chihshang fault and that the surface trace of the fault is approximately consistent with the foothill road. The values between the benchmarks indicate the measurement of horizontal distance changes. The GPS displacement vectors are with respect to a continuous GPS station SHAN in the Longitudinal Valley. For further explanation, see Figure 3.

depth. Finally, minor synclinal folding occurred in the footwall between point 14 and point 7. Through days 120–125 after the earthquake in mid-April 2004, the combined coseismic and postseismic deformation produced about 1.7 cm of vertical offset and 1.1 cm of horizontal shortening over a distance of 40 m between these two benchmarks.

[18] In addition to the thrust faults and the associated fold, arrays of vertical fissures have been observed at the top of the 20-m-high scarp and also can be noticed from results of the geodetic surveys. These fissures, which are generally parallel to the N-S striking major fault, are located around points 1 and 11. The EDM distance-angle measurements imply left-lateral movement of about 6.5 mm and extension of about 10 mm in the two periods. The extension is interpreted as being related to opening of the fissures. We noted in the field that points 1 and 11 were affected not only by these vertical transtensional fissures but also by other nearby arrays of cracks that may result from slope failure at the edge of the slope. Leveling data confirmed relative subsidence of points 1 and 11, as compared with the neighboring points (Figures 5b and 5c). Comparing the

Surface rupture at the Nanhai channel site
fractures

Figure 7. Photographs of surface fractures of the 2003 earthquake on concrete retaining walls and water channels at the Nanhai channel site. (a) Fractures (preexisting) between bridge and midstream water channel. (b) Fractures (preexisting) at the western end of the downstream water channel, (c) Fractures (newly formed) between the bridge and downstream water channel. Circles on the wall mark the locations of nails for measurements of offsets. Note that the fractures usually occurred around the joints between two civil constructions.

measurements of the first and second periods, we found that subsidence occurred mainly during the first period, in association with coseismic slip and shaking that occurred during the December 2003 Chengkung earthquake.

5. Nanhai Channel Site

5.1. Prior to the Chengkung Earthquake

[19] The Nanhai channel site is located at the foot of the Chihshang fault thrust scarp, about 700 m south of the Tapo slope site (Figures 2 and 6). Before the 2003 Chengkung earthquake, creeping ground ruptures of the Chihshang fault were observed in civil constructions at the site. For example, back thrust–type fractures on older retaining walls of the downstream channel exhibited not only E-W compression but also horizontal shortening of about 2 cm/yr, from 1991 to 1993 [*Lee*, 1994; *Angelier et al.*, 1997]. A new concrete wall of the water channel was built in 1994, and like the Tapo slope site, it prevented rupturing at this location. In 1996, new fractures developed in the retaining walls in the midstream channel, which remained unrepaired. Deformation caused by shortening was concentrated at the junction between the midstream water channel and a bridge on the foothill road that separates the water channel into midstream and downstream segments (Figure 6). In addition, significant deformation was also discovered at the western end of the downstream channel that occurred since 2001, about 100 m west of the bridge, where it merges into a larger channel.

[20] In 1998, prior to the Chengkung earthquake, we established a dense geodetic network consisting of 12 benchmarks (Figure 6), located mostly on retaining walls of the WNW-ESE trending water channels, across the fault scarp and the zone of surface fractures over a distance of about 150 m. Leveling and the EDM distance-angle (trilateration and triangulation) measurements were undertaken once or twice a year since 1998. Three benchmarks (points Z, C, and I) were also measured using campaign GPS at the same time. Previous geodetic surveys completed before the 2003 Chengkung earthquake indicated continuous reverse fault movement at a creeping rate of 3 cm/yr, with a horizontal shortening of 2 cm/yr and a vertical movement of 2.2 cm/yr, from 1998 to 2003 [*Lee et al.*, 2003b].

5.2. Deformation of the Chengkung Earthquake

[21] During our field investigation of the 2003 Chengkung earthquake, we found that fresh ruptures had reactivated the aforementioned ruptures at three locations at the Nanhai channel site. These superimposed ruptures developed at (1) the junction between the bridge and the midstream channel (Figure 7a), (2) the western end of the downstream channel (Figure 7b), and (3) the location of the previous back thrust–type fractures in the newly built downstream wall near the bridge (Figure 7c).

[22] Results of the first geodetic survey following the 2003 event, defined by fixing the westernmost footwall benchmark point Z, indicates maximum vertical offset of about 6.4 cm across the fault zone from leveling, and a maximum horizontal displacement of about 5.7 cm along the NW direction (N319°E) at the easternmost point I from GPS (Table 1 and Figures 6 and 8). Displacements during

Nanhai Channel
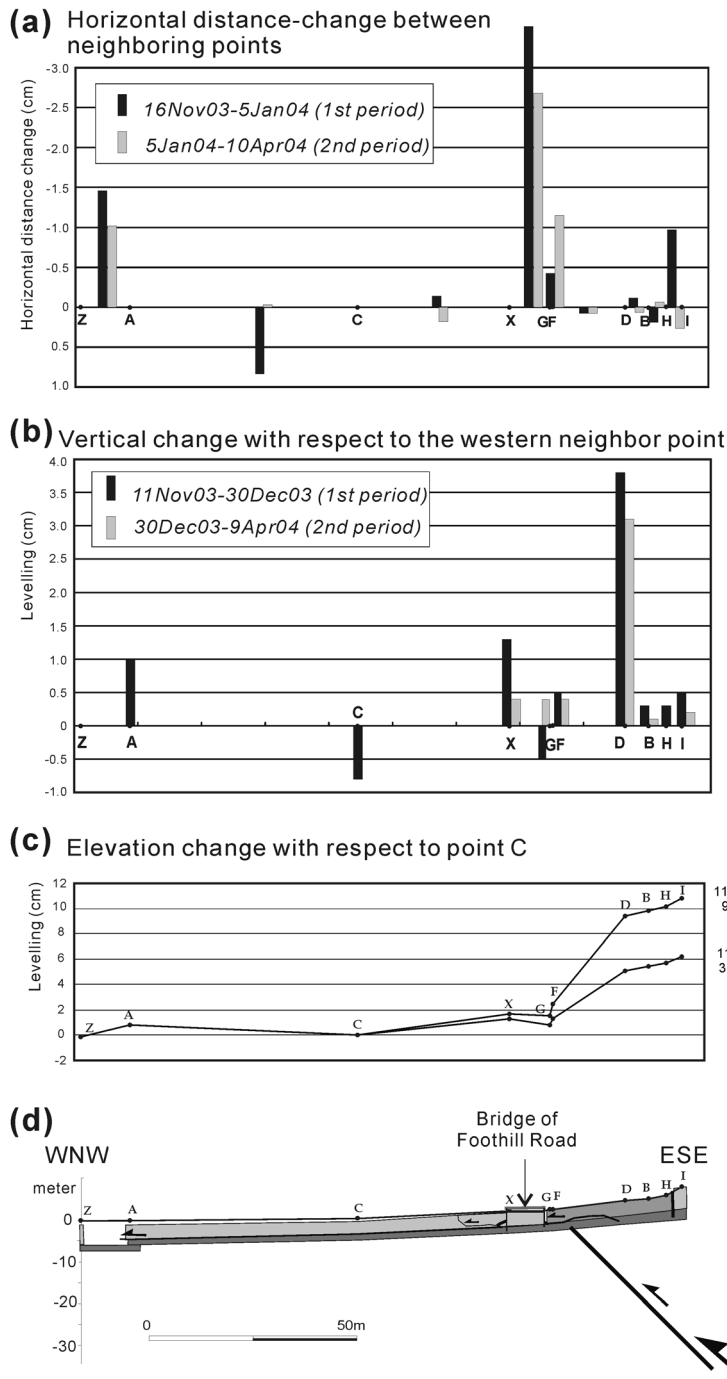
Figure 8. Results of distance-angle and leveling measurements across the surface fault zone of the Chihshang fault and geological interpretation at Nanhai channel site. (a) Horizontal distance change between neighboring points. (b) Vertical change between benchmarks. (c) Elevation changes or vertical movements of benchmarks with respect to the point C. (d) Cross section showing surface ruptures, geometry of the fault, and slip model at the surface level. For further explanation, see Figure 5.

the period 120–125 days after the earthquake increased to 11.0 cm for the maximum vertical offset with 10.7 cm of horizontal slip along the N316°E direction. Measurements at this site suggested that the amount of vertical offset was similar to horizontal shortening (Figure 8). Significant postseismic slip occurred. We also found that some deformation occurred only in the first period, including: (1) significant horizontal shortening between points H and I, (2) horizontal extension between points A and C, and (3) substantial vertical movements at the benchmarks points A, C, and X (Figure 8). Explanations will be given below.

[23] The tip of the principal fault is interpreted to be located near the base of the 20-m-high topographic scarp, which is generally along the NNE trending foothill road (Figures 6 and 8). Because the vertical displacement data from our leveling surveys show a continuous increase toward the hanging wall, with a dramatic increase near surface tip between point F and point D, and a much gentler increase away from the surface tip between point D and point I (Figures 8c and 8d), we interpret the fault as having been partially locked (or coupled) at shallow levels, especially at the very shallow part which have been strongly coupled. The dip angle of the principal fault is estimated to be about 45°, based on the 1:1 ratio between the vertical and horizontal components of displacement across the hanging wall. On the basis of vertical projection of point I, the highest point of elevation changes, we estimate the depth of the coupled segment, on which the fault slip decreased significantly upward, to be at least 25 m below the surface. However, the precise depth cannot be ascertained because of the limit of our baseline on the hanging wall. On the other hand, the depth of the strongly coupled segment is estimated to be less than 15 m, according to the vertical projection of point D. Folding is expected to be the predominant deformation mechanism for the 2003 earthquake near the surface, especially in the hanging wall above the depth of the coupled segment. However, the horizontal shortening was mostly accommodated by three or four brittle ruptures on the retaining walls, as indicated by EDM distance measurements (Figure 8a). We interpret these multiple fractures as a brittle response of horizontal shortening in the concrete water channel above the fault zone.

[24] Some details of the deformation that occurred during the two periods deserve attention. During the first period, 1.0 cm of horizontal shortening occurred at the junction between the upstream and midstream channels (between points H and I), 1.5 cm at the end of the downstream channel (between points Z and A), and 4.0 cm across the bridge (between points X and F). It is interesting to note that the concrete lined water channel acted as an important strain guide with the downstream retaining wall detached from its upper and lower concrete pavements, as indicated by fractures. Because point X is located on the road near the bridge (which has been detached from the water channel), the horizontal shortening between points X and F represent the combined 4.0 cm shortening of the two fractures on both sides of the bridge (Figure 8). As for the vertical movement during the first period, it was revealed by two types of deformation. One type was associated with brittle ruptures in concrete retaining walls, such as the vertical offset on fractures between point A and point X. The other type of deformation was accommodated by folding on the hanging wall of the principal fault (see increasing uplift from point F to point I in Figure 8) without visible ruptures.

[25] During the second set of measurements, the horizontal shortening was marked by progressive fracturing of concrete water channels. Horizontal shortening across the bridge between points C and F was 3.6 cm. At the end of the downstream channel (between points Z and A), the shortening was 0.8 cm. We note that the junction between the midstream and upstream channels (between points H and I)

did not show horizontal movement during the second period, as had occurred during the first period. This first period of shortening at the concrete junction was probably due to coseismic motion. As for the vertical movement, continuous uplift occurred and increased toward the hanging wall. In addition, a significant amount of uplift was concentrated near the surface tip of the main fault, between points F and D. Consistent with the observations discussed above, relative uplift at points A and X did not occur during the second period as had occurred during the first period (Figure 8). As a consequence, we interpret relative uplift of points X and A as being the result of abrupt coseismic strain in the fractured concrete water channel.

[26] From the combined horizontal and vertical displacements, we infer that the principal strand of the Chihshang fault was partially coupled (or locked) and accumulated substantial strains near the surface during the coseismic slip. The coseismic surface deformation was characterized by hanging wall folding and surface rupture near the fault tip. Following the main shock rupture, the accumulated strain was gradually released by rapid postseismic creep. Postseismic surface deformation was thus characterized by hanging wall folding and progressive rupturing along preexisting fractures on man-made construction.
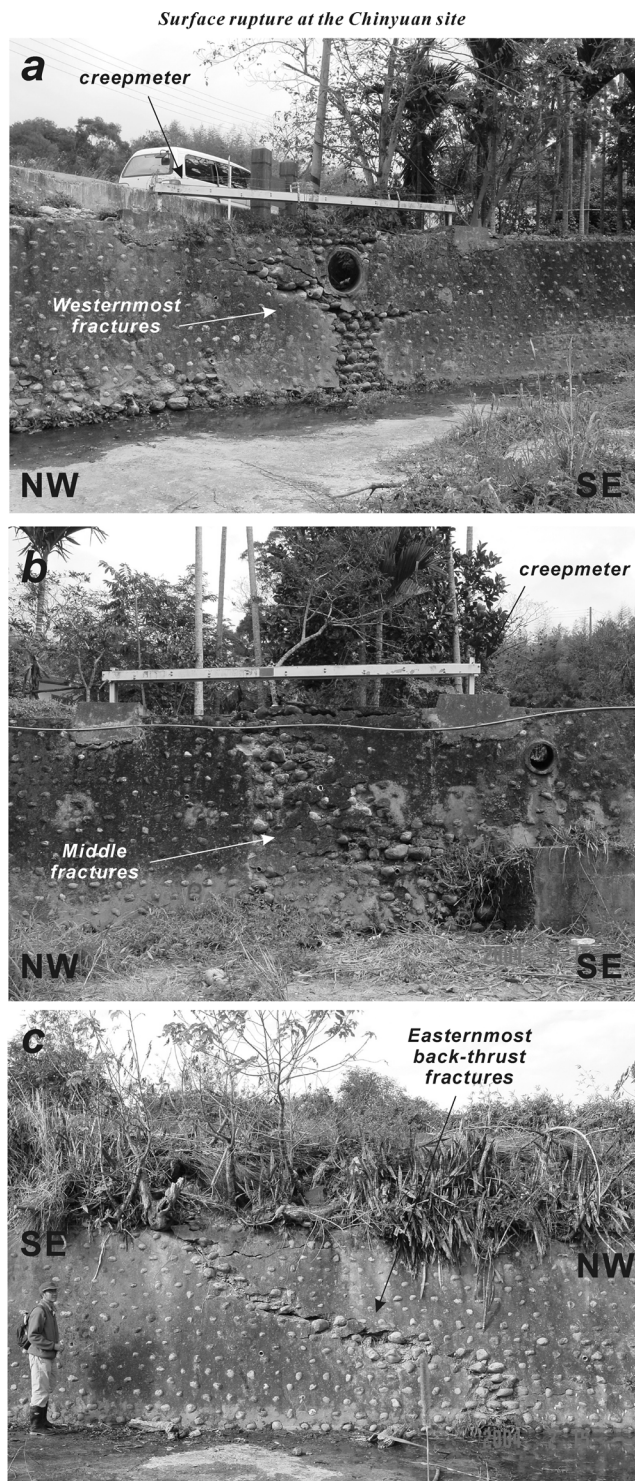
6. Chinyuan Site

6.1. Prior to the Chengkung Earthquake

[27] The Chinyuan site is located across a small alluvial fan in the village of Chinyuan, about 1 km south of the Nanhai channel site along the surface trace of the Chihshang fault (Figure 9). Surface rupture of the Chihshang fault caused by continuous creep in the last 15 years has been documented at several locations in Chinyuan, including cracks in houses, fissures in concrete pavements, and fractures in retaining walls [Chu et al., 1994; Angelier et al., 1997, 2000]. Along an E-W to NW-SE trending concrete water channel, ruptures on the Chihshang fault gave rise to at least three thrust-type fractures in concrete retaining walls and water channel over a distance of about 100 m (Figures 9 and 10). Measurements of progressive offsets in these walls [Angelier et al., 2000] and data from creep meters straddling the three fractures [Lee et al., 2003a] indicate continuous but decreasing creep on all three fractures at a collective horizontal shortening rate of 2.2–2.5 cm/yr from 1992 to 1999 and 1.5–2.0 cm/yr between 2000 and the 2003 Chengkung earthquake [Angelier et al., 2000; Lee et al., 2005]. This implies a deficit of strain release before the Chengkung earthquake, which we have discussed in detail in a separate paper [Lee et al., 2005].

[28] We established a small geodetic network at Chinyuan in 2000, comprising 17 benchmarks along the water channel across the fault zone over a distance of 250 m (Figure 9). As for the two previous sites, systematic campaigns of leveling and distance-angle (trilateration and triangulation) measurements were undertaken once or twice a year between 2000 and 2003. GPS measurements of three benchmarks (points I, Z, and A, Figure 9) were also completed at the same time as the network measurements. Previous geodetic measurements from 2000 to 2003, before the Chengkung earthquake, indicate continuous movement with a creeping rate of about 2–2.5 cm/yr, partitioned into 1.3 cm/yr of uplift

Figure 9. Geodetic network and results of horizontal distance changes and GPS horizontal displacements related to the 2003 Chengkung earthquake at the Chinyuan site. Contour lines show that the site is located on a small alluvial fan (marked in grey dots). The values between the benchmarks indicate locations of measurement of horizontal distance changes. The GPS displacement vectors are with respect to a continuous GPS station SHAN in the Longitudinal Valley. For further explanation, see Figure 3.

and 1.5–2.0 cm/yr of horizontal displacement [*Lee et al.*, 2003b].

6.2. Deformation of the Chengkung Earthquake

[29] During field investigations completed after the 2003 earthquake, several traces of increased rupture were found that reactivated each of the three preexisting fractures in the retaining walls of the water channel (Figure 10). In addition, newly formed hairline cracks were discovered in channel walls further upstream and downstream (outside our existing geodetic network).

[30] Geodetic measurements reveal eastward increasing vertical offset and horizontal shortening across the fault zone at the Chinyuan site (Figure 11). With respect to benchmark point I on the footwall, leveling measurements show a maximum vertical offset of 3.5 cm, and the GPS data indicate a horizontal displacement of 3.0 cm in the NW direction (N318°E), across the fault zone at point A

Surface rupture at the Chinyuan site

Figure 10. Photographs of the surface fractures of the 2003 earthquake on the concrete retaining walls and the water channels at the Chinyuan site. Note that the fractures have been superposed on the preexisting fractures, on which creep meters had been installed in 1998. Photograph locations are shown in Figure 9. (a) Westernmost fractures. Distorted tube indicates horizontal shortening. (b) Middle fractures showing uplift and shortening on the top of retaining wall. (c) Easternmost fractures showing back thrust–type feature.

during the first measurement period (Table 1). The total maximum displacement reached 6.5 cm of vertical offset and 7.0 cm of horizontal slip (in the N302°E direction) during the two measurement periods. Characteristics of the deformation at this site are summarized as follows: (1) Continuous uplift and shortening occurred across the fault zone especially in the hanging wall; (2) the amount of deformation measured, especially during the first periods, was significantly smaller than that obtained from the other two sites, which implies that the Chinyuan site accommodated greater postseismic slip, with respect to the two sites discussed above along the same Chihshang fault; (3) whereas vertical displacements were more smoothly distributed on the hanging wall in comparison with other sites, horizontal shortening was concentrated across specific fracture zones, especially along preexisting fractures in the concrete water channel; (4) for each period, the amount of vertical motion across the fault zone was similar to the horizontal motion; and (5) the differences in behavior between the movements of the first and second periods are minor and resulted mainly from different portions of horizontal shortening distributed in the three fracture zones.

[31] On the basis of field observations and geodetic measurements, the surface tip of the main fault of the Chihshang fault appears to be located between points Z and L (Figure 11). The dip angle of the main fault is about 40°–45° on average within the network, as estimated from the ratio between the vertical and horizontal displacements from point L to point A. A back thrust or back fold structure deformed the surface between points C and D, about 50–60 m east of the surface trace of the main fault. Continuous and smooth uplift in the hanging wall across the fault zone indicates that the fault is strongly, if not totally, coupled near the surface (Figure 11). This also implies that folding is a predominant deformation mechanism in the hanging wall. In addition, because uplift did not stop at an end of the network (point A) and likely extended farther east, the depth of the coupled (or locked) segment, on which the slip on the fault plane decreased significantly toward the ground surface, is estimated to be more than 100 m, according to vertical projection of point A from ground surface to the fault plane (Figure 11). Therefore a future extension of the network toward the hanging wall side is necessary to better constrain the locking depth. Like the Nanhai Channel site, elevation changes showed a dramatic increase across the surface tip of the fault in the hanging wall, between point L and point E (Figure 11). We interpret that a stronger coupling occurred at the very shallow part of the fault, whose depth is estimated to be about 40–50 m, based on vertical projection from point E to the fault plane.

[32] Similar to the water channel at the Nanhai site, measured horizontal shortening was mostly absorbed in retaining walls by brittle fracturing. Along the water channel, horizontal shortening was mainly accommodated along three zones of preexisting thrust-type fractures. Combining data from geodetic measurements and the continuously recorded creep meters (Figure 12), the history of horizontal shortening on fractures during the Chengkung earthquake suggests very limited coseismic horizontal shortening during the main shock, 0.2 cm on the western fracture,
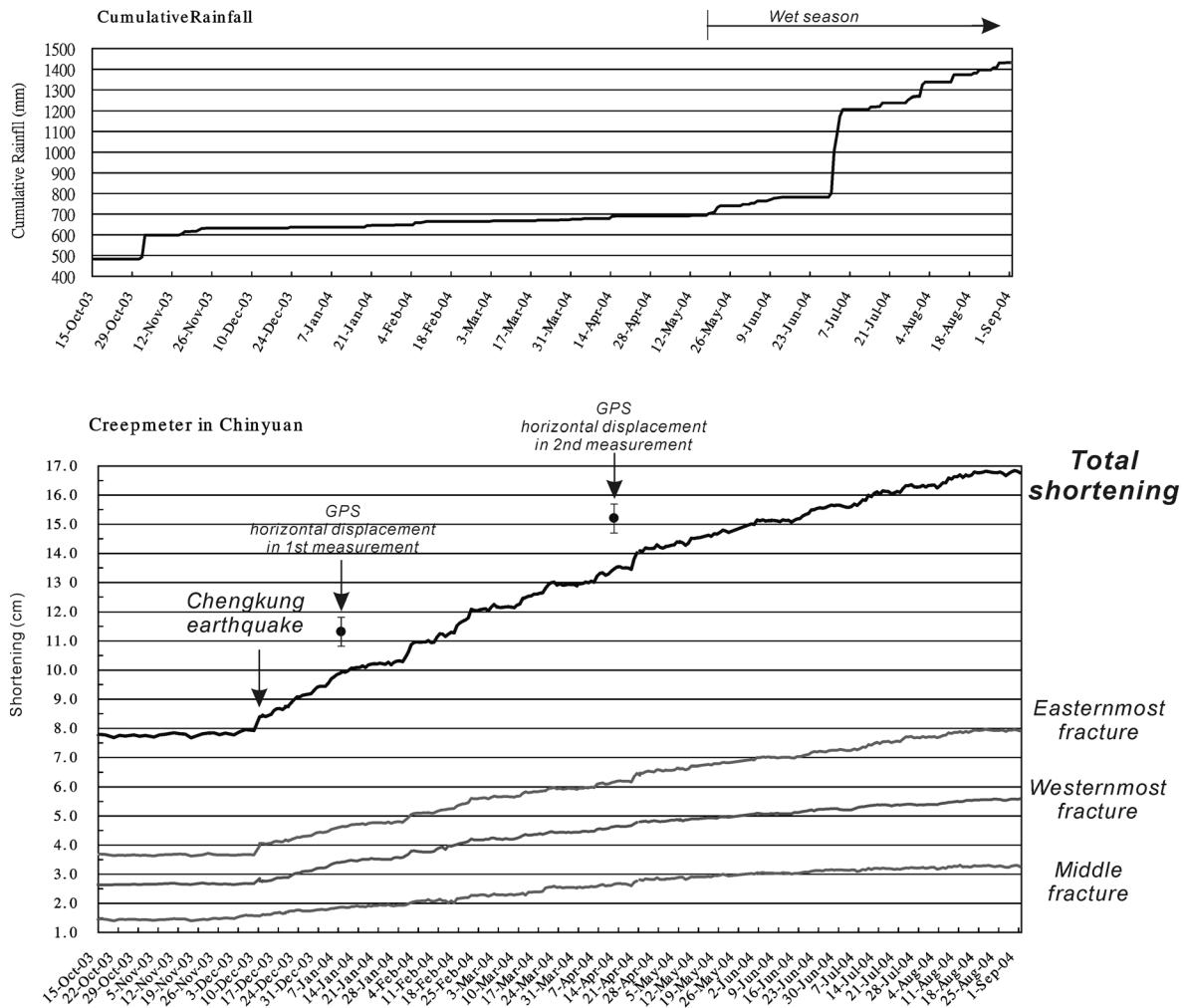
Chinyuan
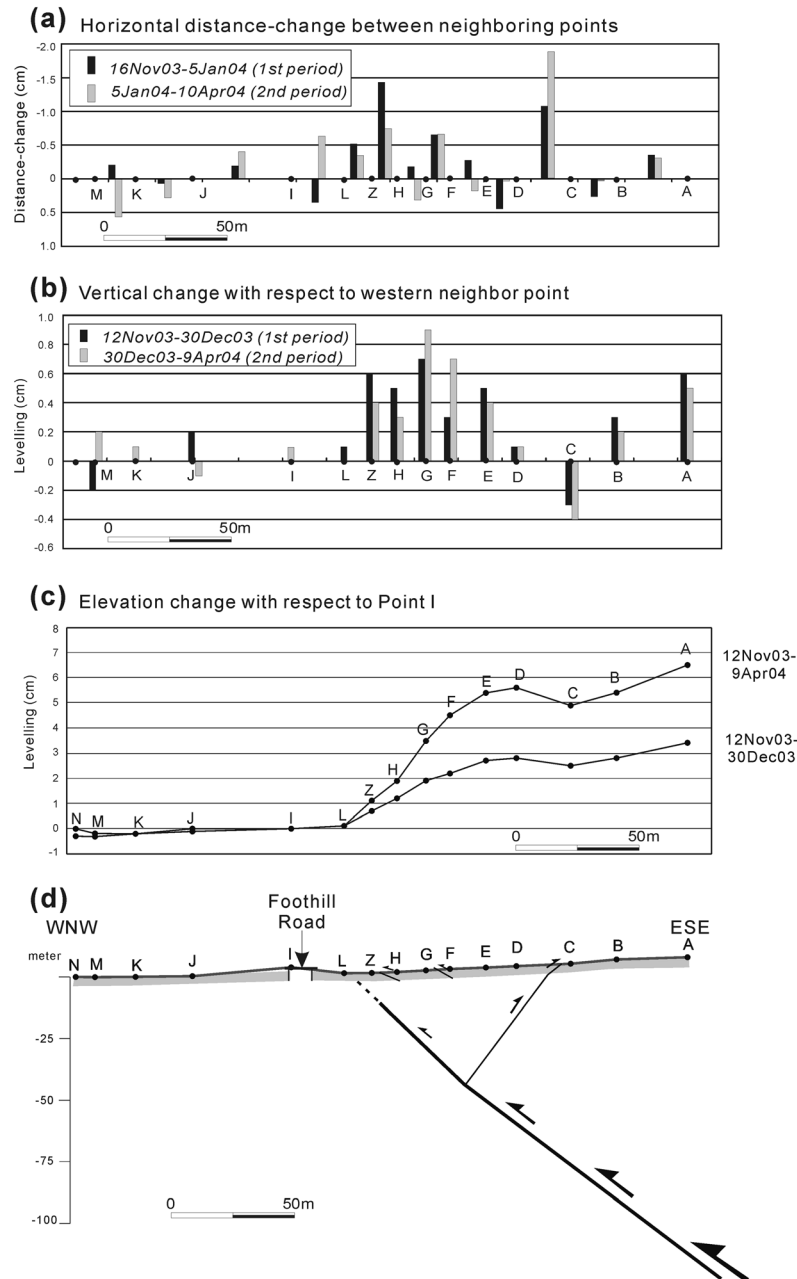
Figure 11. Results of distance-angle and leveling measurements across the surface fault zone of the Chihshang fault and geological interpretation at Chinyuan site. (a) Horizontal distance change between neighboring points. (b) Vertical change between benchmarks. (c) Elevation changes or vertical movements of benchmarks with respect to the point I. (d) Cross section showing surface ruptures, geometry of the fault, and slip model at the surface level. For further explanation, see Figure 5.

undetectable amount (0.0 cm) on the middle fracture, and 0.3 cm on the eastern back thrust–type fracture. Following the main shock, significant and progressive postseismic creep was recorded for more than 8 months. For instance, during the first period (i.e., 25 days following the main shock), horizontal shortening measured on the western fracture reached 0.7 cm, and 0.3 cm on the middle preexisting fracture zone, while slip on the eastern, back thrust–type fracture increased to 0.9 cm. During the

second period (26 to 125 days after the main shock), horizontal shortening on the fractures was 1.3 cm, 0.8 cm, and 1.6 cm for the western, middle, and eastern preexisting fractures, respectively.

[33] GPS measurements across the three-fracture zone indicate horizontal displacement of 3.0 cm during the first period (Figure 12), which is larger by a factor of 1.6, comparing to the collective shortening of 1.9 cm registered by the three creep meters. For the second period, GPS data

Figure 12. Horizontal shortening from creep meters across the surface fractures at the Chinyuan site. The M_w 6.5 Chengkung earthquake showed a combined coseismic horizontal shortening of about 5 mm on three creep meters at this site. Cumulative rainfall data are shown on top of the creep data for comparison. Horizontal displacements across the fault zone from GPS measurements (point A with respect to point I) during the first and second geodetic surveys are shown as dots on Figure 12.

indicate 3.9 cm across the three-fracture zone, which is almost identical to the total shortening of the creep meters in the same period. We interpret that the fractures on the retaining walls reveal a different viscoelastic response to the whole deformation across the surface fracture zone of the Chihshang fault. By the difference of creep meter and GPS displacements during the first period, we estimate the coseismic horizontal displacement across the surface fracture zone to be about 1–2 cm.

7. Summary and Discussion

7.1. Summary of Geodetic Network Measurements

[34] Despite local differences between sites analyzed along the Chihshang fault, our results reveal striking similarities in fault behavior, which define near-surface coseismic and postseismic strain. Comparison of measurements during different periods has implications for how coseismic and postseismic deformations are accommodated in the near surface.

[35] With few exceptions, the observed ground ruptures of the 2003 Chengkung earthquake reactivated preexisting fractures in cement lined channel or retaining walls. These fractures demonstrated fault creep movement before the earthquake on the basis of previous surveys. According to benchmark measurements, earthquake displacements increased gradually across the fault zone at a distance from between 50 and 100 m, especially in the hanging wall of the fault. Deformation associated with the Chengkung earthquake indicates that the fault showed strongly elastic coupling at a shallow depth. The estimated depths of the coupled (or locked) segments, on which the slip of fault decreased significantly upward, range from near 25 m (Nanhai Channel) to more than 100 m (Chinyuan), a determination with large uncertainties that cannot be resolved at this stage because of limited coverage of the geodetic networks.

[36] The displacements also produced anticlinal folding in the hanging wall and lesser synclinal folding on the footwall. Ground fractures that affected civil constructions

Table 2. GPS Measurements of Benchmarks Across the Chihshang Fault at Three Sites (Tapo Slope, Nanhai Channel, and Chinyuan) and Comparison of Three Nearby Continuous GPS Stations (SHAN, TAPE and TAPO) for the 2003 Chengkung Earthquake[a]

|	V, cm	H, cm	Azimuth, deg
Tapo Slope			
Point 8 (footwall)			
First period	2.4	0.9	291
Second period	−0.9	1.7	280
Total	1.5	2.6	283
Point 11 (hanging wall)			
First period	6.4	-	-
Second period	3.0	-	-
Total	9.4	17.7	315
Nanhai Channel			
Point Z (footwall)			
First period	2.4	2.9	301
Second period	−0.9	0.9	198
Total	1.5	2.9	282
Point C			
First period	2.6	4.6	299
Second period	−0.9	0.6	180
Total	1.7	4.3	292
Point I (hanging wall)			
First period	8.8	8.6	313
Second period	3.7	4.6	303
Total	12.5	13.2	309
Chinyuan			
Point I (footwall)			
First period	2.4	3.6	306
Second period	−0.9	0.9	193
Total	1.5	3.3	291
Point Z			
First period	3.1	3.5	315
Second period	−0.5	2.3	203
Total	2.6	3.4	277
Point A (hanging wall)			
First period	5.8	6.5	311
Second period	2.2	4.2	278
Total	8.0	10.3	298
Continuous GPS			
TAPE (footwall)			
First period	2.4	3.4	304
Second period	−0.9	1.5	259
Total	1.5	4.6	290
TAPO (Hanging Wall)			
First period	8.7	11.3	325
Second period	3.6	4.5	325
Total	12.3	15.8	325

[a]The continuous GPS station SHAN at the town of Chihshang at the footwall in the Longitudinal Valley is selected as the referenced point. The standard deviations of the GPS measurements are about 1 cm and 0.3 cm, for vertical (V) and horizontal (H) components, respectively. Note that the westernmost points in each geodetic network are given the same vertical offset as the continuous GPS station TAPE (which is 20–30 m away from the surface trace of the fault), because of large uncertainty of vertical component in GPS campaign measurements. Leveling data are then adopted for other points in the geodetic networks but referenced to the westernmost points.

were located not only near the surface tips of both the main fault and the back thrust (back fold), but also at junctions between different constructions (e.g., bridge versus wall) where concrete structures acted as strain guides. It is common for concrete civil structures to undergo localized deformation that originate as fractures or other strain distributed over a wide zone near surface rupture zone of an earthquake [*Kelson et al.*, 2001]. Our observations also suggest that the subhorizontal concrete walls respond to horizontal shortening in a more brittle way, whereas vertical uplift is mostly accommodated by elastic folding. Brittle

failure and deformed behavior on man-made structure deserve special attention for seismic hazard evaluation and mitigation.

7.2. Lateral Spreading and Gravitational Effect

[37] The results of the geodetic measurements show that extensional cracks occurred near the top of the scarp at Tapo Slope, the only site situated on a substantial slope surface. As mentioned above, field evidence showed slumping with a few vertical fissures, which were subparallel to the scarp or the strike of the fault, around two benchmarks (points 1
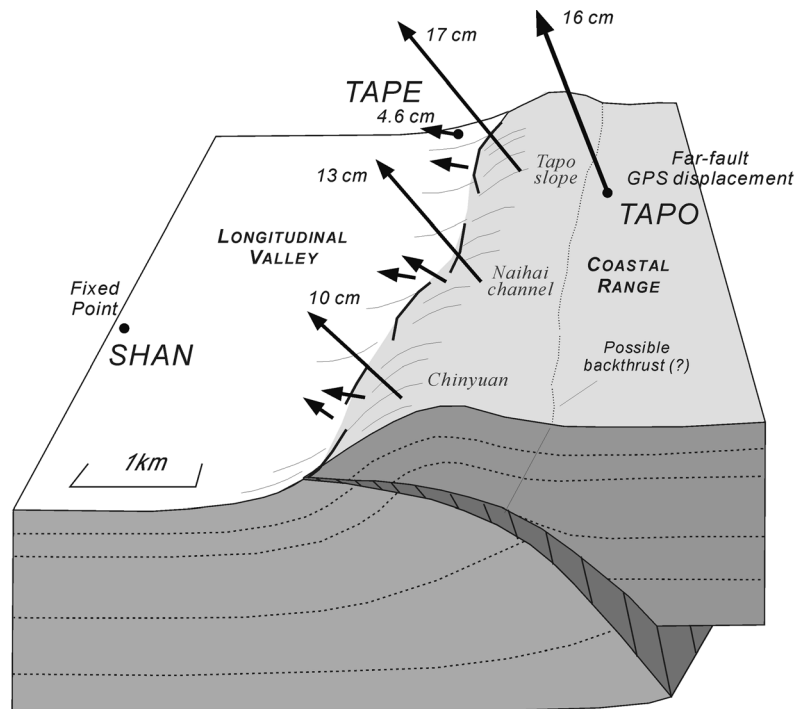
Figure 13. Schematic fault movement and deformation across the Chihshang fault related to the 2003 Chengkung earthquake (modified from *Angelier et al.* [2003]). The GPS horizontal vectors, which are with respect to a fixed point of the GPS continuous station (SHAN) on the footwall, indicate strain concentrated near the fault as well as more distributed far-fault deformation.

and 11) near the top of the slope. Leveling measurements revealed substantial subsidence for these two benchmarks relative to the neighboring benchmarks (about 0.5 cm for point 1 and 3 cm for point 11 throughout the two periods of survey).

[38] Elsewhere, field observations also found that vertical fissures with minor offsets commonly occurred along the scarps of the Chihshang fault, especially in the mudstone of the Lichi mélange [*Angelier et al.*, 1997, 2000; *Chang et al.*, 2003]. These fissures generally trend subparallel to the strike of the Chihshang fault as well to the slope of the scarps. We infer that these vertical fissures are related to the combined effects of extension induced by uplifting or folding in the hanging wall of the fault [*Philip et al.*, 1992] and lateral spreading triggered by earthquake shaking and gravitational sliding.

7.3. Comparison With Far-Field GPS Measurements

[39] In order to better investigate and distinguish near- and far-field fault effects as well as influence of the response of unconsolidated deposits at local sites, we compared GPS measurements of the three geodetic networks with that available far field GPS data. Data from three continuous GPS stations operated by the Central Weather Bureau–Institute of Earth Sciences, Academia Sinica (CWB-IES) program were especially important in the Chihshang area. One station (SHAN) is located in the footwall of the fault southwest of the town of Chihshang, about 2–3 km west of our sites (see location in Figure 2). One station (TAPE) is located in the footwall very close (about 20–30 m) to the fault scarp. The other station

(TAPO) is located in the hanging wall, about 700 m east of the surface trace of the Chihshang fault.

[40] By taking the far-field footwall GPS station SHAN as a fixed reference point, data from the geodetic networks of the three sites and continuous stations TAPE and TAPO were incorporated in an analysis of the near- and far-field displacements across the Chihshang fault (Table 2 and Figure 13). GPS measurements in the geodetic networks show gradual and significant change in both amount and direction of the displacements within a short distance across the fault zone. This is consistent with our interpretation that folding is the predominant deformation mechanism at shallow level. Note that the vertical offsets shown in Table 2 are a combination of GPS measurements and leveling data. Because of the great uncertainty in the vertical components deduced from GPS campaign measurements, we do not use these data as a final result of vertical offsets for benchmarks in the geodetic network. Instead, we take the footwall continuous GPS station TAPE as the vertical reference point. The westernmost points in the three geodetic networks are adopted to be the same vertical offset as the station TAPE. Vertical offsets of other points in the geodetic network then were calculated from the leveling results by comparing to the westernmost point for each network.

[41] Comparing the far-field to the near-fault measurements, moderate but significant deformation occurred outside of the fault zone covered by our geodetic networks. About 2.6–3.3 cm of additional horizontal displacement and 1–2 cm of vertical offset occurred in the footwall between the far field station SHAN and the westernmost
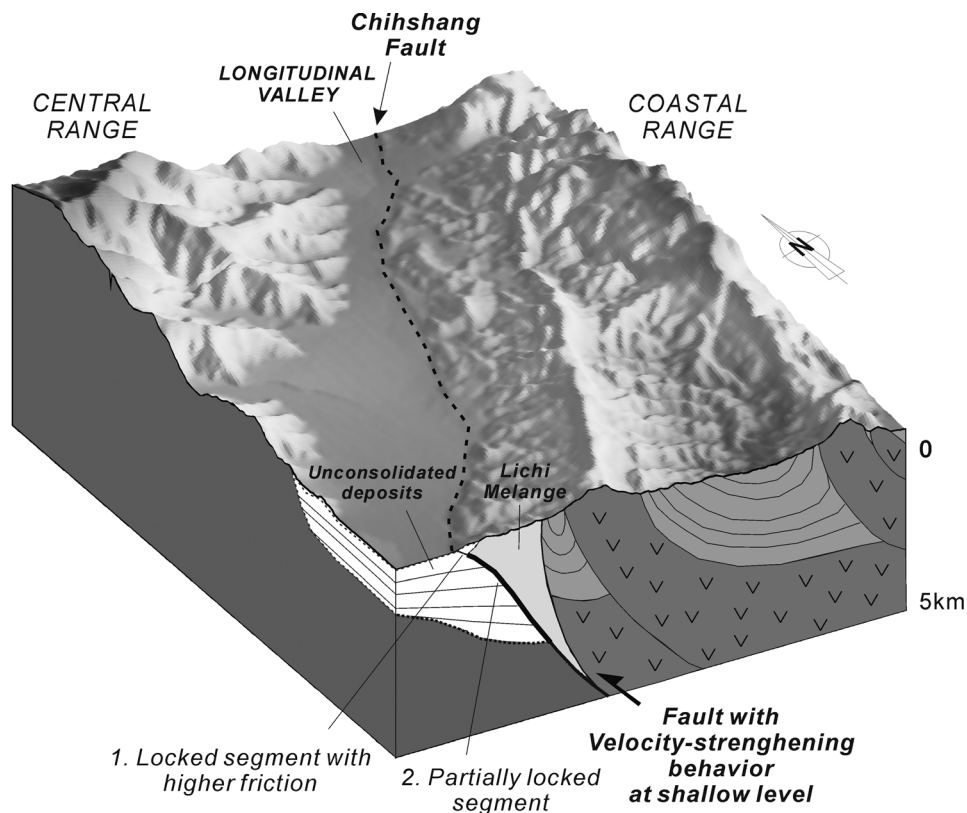
Figure 14. Block diagram illustrating the geological context across the Chihshang fault. Unconsolidated deposits and/or mudstone of the Lichi mélange that may behave in a viscoelastic fashion are interpreted to cause the strongly to partially coupled fault at shallow depth.

benchmarks of the networks (Figure 13). This indicates that the alluvial deposits in the Longitudinal Valley absorbed substantial shortening within a distance of 2–3 km from the Chihshang fault. Because there is no evidence of surface faulting in this zone of rather flat land (where many concrete constructions likely would have recorded fracturing), we interpret this to suggest that deformation may be accommodated by ductile or elastic strain in the thick sequence of unconsolidated alluvial deposits in the Longitudinal Valley (Figure 14).

[42] The horizontal displacements at the far field hanging wall station TAPO is larger than those at the easternmost benchmarks of the networks (Table 2 and Figure 13), except for the Tapo slope site where the benchmark point 11 experienced lateral spreading. Furthermore, the strike-slip component (left-lateral slip) of the far field station TAPO is higher than the benchmarks near the fault network. On the other hand, the vertical displacement at TAPO station is slightly smaller than the easternmost benchmarks of the Nanhai channel networks. These together indicate that substantial deformation, including shortening of 2–6 cm, left-lateral slip, and maybe a little vertical subsidence, occurred in the hanging wall over a distance of about 600 m between the geodetic networks and TAPO station. This can be interpreted to suggest that a back thrust (or back fold) of the Chihshang fault may exist in this region (Figure 13).

[43] GPS data thus indicate that the deformation zone of the Chihshang fault occurs over a wider area than our

geodetic networks. The fact that the increasing displacement amounts extended continuously eastward beyond the eastern bounds of our networks also implies that the geodetic networks are not large enough to cover the whole deformation zone, although they recorded most of the deformation, including the most obvious active fractures. For example, at the Nanhai channel site, baselines in the network are relatively short in the hanging wall side. The network was not extended to the top of the geomorphic scarp of the Chihshang fault, because dense vegetation precluded line of sight measurements. As for the Chinyuan site, we speculate that the deformation zone is relatively wider, because the region is located in an alluvial fan, with a sequence of unconsolidated deposits across the fault zone [*Chow et al.*, 2001]. These unconsolidated deposits provide a typical mechanical behavior of velocity strengthening (stabilizing) and thus implying strong coupling for the fault slip during earthquake [*Marone et al.*, 1991]. That, in turn, explains why the surface deformation zone is wider at the Chinyuan site and why the site has more significant postseismic slip.

7.4. Postseismic Slip and Geological Implications

[44] A significant part of the measured deformation across the surface fault zone for the 2003 earthquake can be attributed to postseismic creep. Combining continuous GPS data, creep meter data, and geodetic network measurements, very limited near-fault deformation is deduced, about 1–2 cm of horizontal shortening and 1–2 cm of vertical offset, during coseismic slip at the surface trace of the

Chihshang fault. Greater deformation, however, can be attributed to postseismic creep. For example, about 8–12 cm of horizontal shortening and 6–11 cm of vertical offset were recorded at the measured sites by April 2004 (combined first and second periods), about 125 days after the earthquake, whereas half of that (4–7 cm) was measured about 20 days after the earthquake (first period). It is worth noting that ratios of postseismic creep to coseismic slip observed at GPS stations decrease as a function of distance to the surface trace of the Chihshang fault. This is revealed by near-field networks and far field GPS observations in the scale of several to tens of kilometers: GPS stations closer to the surface trace of the Chihshang fault recorded higher ratios of postseismic slip versus coseismic slip with respect to the stations farther away [*Chen et al.*, 2006], along the line perpendicular to the NNE striking Chihshang fault. We interpret this to suggest that postseismic creep on the Chihshang fault plane is larger at the shallow level than that at deeper levels. Thus the ratio of postseismic to coseismic slip decreases as a function of depth of the fault.

[45] As for the distribution of coseismic slip during the Chengkung earthquake, the half-space elastic inversions of either GPS data [*Ching et al.*, 2004] or the surface motion data from seismometers [*Cheng et al.*, 2004] suffice to indicate that the 2003 coseismic slip on the Chihshang fault was up to 80–100 cm near the hypocentral area at a depth of 10–25 km, decreasing dramatically to only 10–30 cm in the upper 5 km. This implies a possible accumulation of coseismic strain at shallow level and also indicates that the shallow part of the fault was strongly coupled, if not totally locked, during the earthquake. We interpret the coupling behavior of the Chihshang fault at shallow levels to depend on the mechanical properties of the sediment layers and rock formations near the surface, which consist of unconsolidated deposits in the footwall and mudstone with sheared fault gouge (the Lichi mélange) in the hanging wall (Figure 14). This interpretation is similar to that of *Marone et al.* [1991], who interpreted earthquake after slip along the San Andreas Fault as a result of velocity strengthening of unconsolidated deposits at shallow level by applying the frictional instability law. Other rock properties, especially pore fluid pressures, might affect slip behavior along a fault zone [e.g., *Irwin and Barnes*, 1975]. However, their investigation is beyond the scope of this paper.

[46] Comparing our measurements from the three sites, the effect of surface materials appear to be more significant at the Chinyuan site. Unlike the other two sites located across a topographic slope, the Chinyuan site is covered by an alluvial fan with thick deposits. Alternatively, the fault zone at the Chinyuan site shows relatively smaller amounts of total displacement compared to the other two sites. Vertical displacements also increased more gradually and slowly (i.e., magnitude of slip) toward the hanging wall side at the Chinyuan site relative to the other two sites. We attribute this difference to the effect of stronger fault coupling and a deeper locked segment near the surface level. Furthermore, the alluvial fan of the Chinyuan site may provide stronger fault coupling than the other two sites where the separates Lichi mélange from Quaternary fluvial deposits (Figure 14). However, the possibility that displacements in the earthquake are not evenly distributed along strike cannot be excluded.

[47] It is worth noting that the Chengkung earthquake occurred during the dry season (Figure 12), when the coupling of the fault slip would have been significantly stronger than that during the wet season, according to the creep meter data collected in five years [*Lee et al.*, 2003a]. The creep meter data from 1998–2003 indicated that surface creep stops during dry season and starts to move rapidly at the beginning of wet season for each year. Compared to seismicity and far-field GPS data, this seasonal variation was interpreted to be an effect at shallow level [*Lee et al.*, 2003a]. The creep meter observation supports our interpretation of strong fault coupling near surface. Because mechanical resistance of these rock formations to frictional sliding dramatically decreases as the water content increases, postseismic creep along the fault would gradually release the coseismic strain stored in the upper few kilometers.

[48] Significant postseismic creep has been observed and documented elsewhere in the world, for example, the 1966 Parkfield earthquake, the 1979 Imperial Valley earthquake, and the 1987 Superstition Hills earthquake [*Scholz et al.*, 1969; *Cohn et al.*, 1982; *Williams and Magistrale*, 1989]. Although these are all strike-slip faults, the postseismic slips are interpreted as strongly related to the occurrence of thick sediments [*Williams and Magistrale*, 1989; *Marone et al.*, 1991]. It is interesting to note that all the above mentioned earthquakes, including the Chengkung earthquake, are of a moderate magnitude about 6.2–6.6. It appears that thick sediments at the shallow level play an important role in providing strong coupling (or velocity strengthening) during the coseismic slip of a moderate earthquake, regardless of whether the fault is strike-slip (such as the Imperial Valley fault) or thrust (such as the Longitudinal Valley fault).

References

Angelier, J., H. T. Chu, and J. C. Lee (1997), Shear concentration in a collision zone: Kinematics of the active Chihshang fault, Longitudinal Valley, eastern Taiwan, *Tectonophysics*, *274*, 117–144.

Angelier, J., H. T. Chu, J. C. Lee, and J. C. Hu (2000), Active faulting and earthquake risk: The Chihshang Fault case, Taiwan, *J. Geodyn.*, *29*, 151–185.

Angelier, J., J. C. Lee, H. T. Chu, and J. C. Hu (2003), Reconstruction of fault slip of the September 21st, 1999, Taiwan earthquake in the asphalted surface of a car park, and co-seismic slip partitioning, *J. Struct. Geol.*, *25*(3), 345–350.

Barrier, E., and H. T. Chu (1984), Field trip guide to the Longitudinal Valley and the Coastal Range in eastern Taiwan, paper presented at Sino-French Colloquium on Geodynamics of the Eurasian-Philippine Sea Plate Boundary, Taipei, 26–30 April.

Bonilla, M. G. (1975), A review of recently active faults in Taiwan, *U.S. Geol. Surv. Open File Rep.*, *75–41*, 72 pp.

Cattin, R., and J. P. Avouac (2000), Modeling mountain building and the seismic cycle in the Himalaya of Nepal, *J. Geophys. Res.*, *105*, 13,389–13,407.

Chang, C.-P., T.-Y. Chang, C. Liu, J.-C. Lee, Y.-B. Tsai, K.-C. Jian, S.-J. Huang, and S.-W. Wu (2003), Surface deformation and mechanism in the Chihshang area, Longitudinal Valley of Taiwan (in Chinese with English abstract), *Bull. Cent. Geol. Surv.*, *14*, 187–198.

Chen, H. H., and R. J. Rau (2002), Earthquake locations and style of faulting in an active arc-continent plate boundary: The Chihshang fault of eastern Taiwan, *Eos Trans. AGU*, *83*(47), Fall Meet. Suppl., Abstract T61B-1277.

Chen, H. Y., S. B. Yu, and L. C. Kuo (2006), Coseismic and postseismic surface displacements of the 10 December 2003 (Mw 6.5) Chengkung, eastern Taiwan, earthquake, *Earth Planets Space*, in press.

Cheng, S. N., Y. T. Yeh, and M. S. Yu (1996), The 1951 Taitung earthquake in Taiwan, *J. Geol. Soc. China*, *39*(3), 267–285.

Cheng, L. W., J. C. Lee, Y. M. Wu, and J. C. Hu (2004), Inversion of coseismic deformation of Chengkung earthquake in eastern Taiwan revealed by strong motion and continuous GPS, *Eos Trans. AGU*, *85*(47), Fall Meet. Suppl., Abstract T13F-06.

Ching, K.-E., R.-J. Rau, and Y. Zeng (2004), Coseismic source model of the 2003 Cheng-Kung, Taiwan, earthquake based on the GPS displacement observations, paper presented at Annual Meeting, Geophys. Soc., Taoyuan, Taiwan.

Chow, J., J. Angelier, J. J. Hua, J. C. Lee, and R. Sun (2001), Paleoseismic event and active faulting: From ground penetrating radar and high-resolution seismic reflection profiles across the Chihshang Fault, eastern Taiwan, *Tectonophysics*, *333*, 241–259.

Chu, H. T., J. C. Lee, and J. Angelier (1994), Non-seismic rupture of the Tapo and the Chinyuan area on the southern segment of the Huatung Longitudinal Valley fault, eastern Taiwan, paper presented at Annual Meeting, Soc. of Geol. of China, Taipei.

Chung, L. H., J. B. H. Shyu, Y. G. Chen, J. C. Lee, and J. C. Hu (2002), Surface rupture reevaluation of the 1951 earthquake sequence and neotectonic implication of east Taiwan, *Eos Trans. AGU*, *83*(47), Fall Meet. Suppl., Abstract T62D-11.

Cohn, S. N., C. R. Allen, R. Gilman, and N. R. Goutly (1982), Preearthquake and postearthquake creep in the Imperial fault and the Brawley fault zone, in *The Imperial Valley Earthquake of October 15, 1979, U.S. Geol. Surv. Prof. Pap.*, *1254*, 161–167.

Ho, C. S. (1986), A synthesis of the geologic evolution of Taiwan, *Tectonophysics*, *125*, 1–16.

Irwin, W. P., and I. Barnes (1975), Effects of geological structure and metamorphic fluids on seismic behavior of the San Andreas fault system in central and northern California, *Geology*, *3*, 713–716.

Kelson, K. I., K.-H. Kang, W. D. Page, C.-T. Lee, and L. S. Cluff (2001), Representative styles of deformation along the Chelungpu fault from the 1999 Chi-Chi (Taiwan) earthquake: Geomorphic characteristics and responses of man-made structures, *Bull. Seismol. Soc. Am.*, *91*(5), 930–952.

Lee, J. C. (1994), Structure et déformation active d'un orogène: Taiwan, Mem. Sci. Terre, 94–17 thesis, Univ. e Pierre et Marie Curie, Paris.

Lee, J. C., and J. Angelier (1993), Location of active deformation and geodetic data analyses: An example of the Longitudinal Valley fault, Taiwan, *Bull. Soc. Geol. Fr.*, *164*(4), 533–570.

Lee, J. C., F. S. Jeng, H. T. Chu, J. Angelier, and J. C. Hu (2000), A rod-type creepmeter for measurement of displacement in active fault zone, *Earth Planets Space*, *52*(5), 321–328.

Lee, J. C., J. Angelier, H. T. Chu, J. C. Hu, and F. S. Jeng (2001), Continuous monitoring of an active fault in a plate suture zone: A creepmeter

study of the Chihshang active fault, eastern Taiwan, *Tectonophysics*, *333*, 219–240.

Lee, J. C., J. Angelier, H.-T. Chu, J.-C. Hu, F.-S. Jeng, and R.-J. Rau (2003a), Active fault creep variations at Chihshang, Taiwan, revealed by creepmeter monitoring, *J. Geophys. Res.*, *108*(B11), 2528, doi:10.1029/2003JB002394.

Lee, J. C., J. Angelier, H. Y. Chen, H. T. Chu, and J. C. Hu (2003b), 3-D kinematics analysis of surface ruptures on an active creeping fault at Chihshang, eastern Taiwan, *Eos Trans. AGU*, *84*(46), Fall Meet. Suppl., Abstract T11F-05.

Lee, J. C., J. Angelier, H. T. Chu, J. C. Hu, and F. S. Jeng (2005), Monitoring active fault creep as a tool in seismic hazard mitigation: Insights from creepmeter study at Chihshang, Taiwan, *C. R. Geosci.*, *337*(13), 1200–1207, doi:10.1016/j.crte.2005.04.018.

Marone, C. J., C. H. Scholtz, and R. Bilham (1991), On the mechanics of earthquake afterslip, *J. Geophys. Res.*, *96*, 8441–8452.

Philip, H., E. Rogozhin, A. Cisternas, J. C. Bousquet, B. Borisov, and A. Karakhanian (1992), The Armenian earthquake of 1988 December 7: Faulting and folding, neotectonics and palaeoseismicity, *Geophys. J. Int.*, *110*, 141–158.

Savage, J. C. (1983), A dislocation model of strain accumulation and release at a subduction zone, *J. Geophys. Res.*, *88*, 4984–4996.

Scholz, C. H., M. Wyss, and S. W. Smith (1969), Seismic and aseismic slip on the San Andreas fault, *J. Geophys. Res.*, *74*, 2049–2069.

Schomaker, M. C., and R. M. Berry (1981), *Geodetic Leveling*, U.S. Dep. of Commer., Washington, D. C.

Suppe, J. (1981), Mechanics of mountain building in Taiwan, *Mem. Geol. Soc. China*, *4*, 67–89.

Suppe, J. (1984), Kinematics of arc-continent collision, flipping of subduction, and back-arc spreading near Taiwan, *Mem. Geol. Soc. China*, *6*, 21–33.

Teng, L. S. (1990), Tectonic evolution of late Cenozoic arc-continent collision in Taiwan, *AAPG Bull.*, *74*, 1004–1005.

Thatcher, W., and J. B. Rundle (1979), A model for the earthquake cycle in underthrust zones, *J. Geophys. Res.*, *84*, 5540–5556.

Tsai, Y. B. (1986), Seismotectonics of Taiwan, *Tectonophysics*, *125*, 17–38.

Williams, P. L., and H. W. Magistrale (1989), Slip along the Superstition Hills fault associated with the 24 November 1987 Superstition Hills, California, earthquake, *Bull. Seismol. Soc. Am.*, *79*, 390–410.

Yü, M. S., H. T. Chu, and C. L. Hsiao (1997), On the geomorphic and recent faulting deformation in the Tapo-Wanan area, eastern Taiwan, *Trans. Jpn. Geomorphol. Union*, *18*, 152–153.

Yu, S. B., and L. C. Kuo (2001), Present-day crustal motion along the Longitudinal Valley fault, eastern Taiwan, *Tectonophysics*, *333*, 199–217.

Yu, S. B., and C. C. Liu (1989), Fault creep on the central segment of the longitudinal valley fault, eastern Taiwan, *Proc. Geol. Soc. China*, *32*, 209–231.

Yu, S. B., H. Y. Chen, and L. C. Kuo (1997), Velocity field of GPS stations in the Taiwan area, *Tectonophysics*, *274*, 41–59.

————————

J. Angelier, Géosciences Azur, Observatoire Océanologique de Villefranche, B.P. 48, Villefranche-sur-Mer F-06235, France.

H.-Y. Chen, J.-C. Lee, and S.-B. Yu, Institute of Earth Sciences, Academia Sinica, P.O. Box 1-55, Nankang, Taipei, Taiwan 115. (jclee@earth.sinica.edu.tw)

H.-T. Chu, Central Geological Survey, P.O. Box 968, Taipei, Taiwan 235.

J.-C. Hu, Department of Geosciences, National Taiwan University, Taipei, Taiwan 106.